

Probabilistic Analysis of Airspace Capacity in Adverse Weather Scenarios

Anastasia Lemetti, Tatiana Polishchuk and
Valentin Polishchuk
Communications and Transport Systems, ITN,
Linköping University (LiU),
Norrköping, Sweden
firstname.lastname@liu.se

Alfonso Valenzuela, Antonio Franco,
Juan Nunez-Portillo and Damián Rivas
Department of Aerospace Engineering,
Universidad de Sevilla,
41092 Seville, Spain
avalenzuela@us.es

Abstract—Accurate prediction of the Air Traffic Control (ATC) sector capacity is a cornerstone in solving the demand/capacity imbalance problem in aviation. In this paper, we develop a methodology, based on the continuous maxflow/mincut theory, to estimate the reduction of the ATC sector capacity due to predicted convective weather activity. The meteorological forecast uncertainty is quantified using Ensemble Weather Forecasting. We demonstrate how to determine congestion in ATC sectors, using an example of a realistic sector, also a whole sector configuration, and propose a way to present the probabilistic overload and congestion status to support the decision-making process at the Flow Management Position.

Keywords—Airspace capacity, congestion, probabilistic weather modeling, convective weather

I. INTRODUCTION

The main task of Flow Management is to achieve the optimum exploitation of the capacities of all Air Traffic Control (ATC) units (in particular, the Area Control Centre, ACC), taking into account the staffing situation of the unit and other impacting factors like weather or technical issues. In this task in Europe, the Flow Management Position (FMP), an operational position located in the ACC Ops Room, monitors the expected traffic in ATC sectors, and adjusts the value of capacity in view of adverse weather conditions, unpredicted staffing shortages, equipment failures, etc. When the FMP detects an excess of traffic over capacity, he/she coordinates possible traffic flow measures both at the ACC and the Network Manager (NM) levels.

The presence of convective cells reduces the airspace available for conflict resolution tasks and makes the traffic irregular and not easy to predict, thus increasing traffic complexity and reducing the capacity of the sector. The provision of an accurate prediction of the development of convective cells inside a sector, a trustworthy forecast and characterization of the future traffic, and a reliable estimation of the impact of the convective weather on the sector capacity would lead the FMP to take anticipated, appropriate, and timely flow measures, which as a consequence will lead to a reduction of delays.

In this paper, we focus on the development of a methodology for forecasting the sector capacity reduction due to convective weather and its application in detection of the sector congestion.

The rest of the paper is organized as follows. In Section II we review related work on the topic. Section III presents the overall framework considered in this paper. Section IV describes the methodology for probabilistic analysis of sector capacity reduction. We describe the case study we use to demonstrate the proposed concept in Section V, and present the example results for this case in Section VI. Section VII concludes the paper and outlines the future work.

II. RELATED WORK

The continuous maxflow/mincut theory [1] is used as the starting point in this work, which extends cornerstone discrete network flow results (maxflow/mincut theorem, Menger's theorem and flow decomposition theorem) to continuous domains. The previous development of this continuous flow theory and algorithms was motivated by ATM needs, and ATM applications of the geometric flow results are presented in [2] and [3]. The prior work on capacity estimation assumed that the obstacles are deterministic, i.e. that their shapes and locations were known exactly. In this work, we extend the capacity estimation to the stochastic setting when the adverse weather zones, defining the obstacles, are given by probabilistic forecasts.

The prior work [4] proposed the methods for establishing dependence of capacity on weather coverage. In this paper, weather coverage is not used as the input; instead, the input consists of an ensemble of weather forecasts. Following [5], we extend the methods from [4] to study the dependence of the capacity on the forecasts spatial and temporal uncertainty.

We take into account the severity of the weather and probabilities of occurrence of the hazardous weather cells supplied by the forecasts. We treat the airspace as a weighted region in which the weight of every point represents the severity and the likelihood of weather hazard at that point. The geographic spread of the mincuts, taken over the ensemble weather forecast, visualizes the spatial pattern of capacity reduction in the sector (probabilistic impact maps in [5]). To quantify the reduction of the capacity (not the capacity itself), we compute the available flow capacity ratio as described in [6].

Nowadays, the FMP monitors the traffic load of each ATC sector via the Collaboration Human Machine Interface (CHMI), a standalone application which provides a graphical

interface to display data [7]. The traffic load is usually measured as the rate of flights predicted to enter the sector in a 1-hour rolling interval, i.e. the entry count, and it is compared with the Monitoring Value (MV) [8]. The MV is the agreed number of flights accepted to enter into a reference location per rolling hour beyond which coordinated actions may be considered. The MV is not the capacity itself, but normally close to 90% of real capacity; thus, if the capacity is reduced, the MV should be reduced in the same proportion. An overload of 3% over MV is not considered as an overload, it starts to be an overload once the load reaches 10% over MV.

The efforts made in the past to predict the congestion of a particular airspace can be grouped into two different approaches: the separate prediction of traffic load and capacity values and then its comparison, or the direct prediction of the congestion status. The first approach is the one followed by the NM, and the one proposed in [9] for a probabilistic methodology. The work presented in [10] follows the second approach to directly predict the activation of ATFM regulations, by using machine learning and historical data. In this paper, we follow the first approach, where probabilistic traffic loads and probabilistic monitoring values are predicted, using the same weather forecasts, and then compared.

III. PROBLEM FRAMEWORK

A. Concept

The framework for this paper is the integration of meteorological (MET) forecast uncertainty into the decision-making process for FMP under adverse weather; in particular, with the provision of probabilistic forecasts of traffic loads, sector complexity, and sector capacity reduction under convective weather for a forecasting horizon of 8 hours. Thus, the focus is on the tactical flow management phase. Given the forecast lead time of 8 hours, and the stochastic evolution of the atmosphere, the predictions on traffic loads, sector complexity, and sector capacity are affected by meteorological forecast uncertainty, so that a probabilistic approach becomes the appropriate one. In this paper we present an analysis of the reduction of sector capacity under convective weather.

B. Characterization of Weather Forecast Uncertainty

In this work, weather forecast uncertainty is quantified using Ensemble Weather Forecasting (EWF) as the probabilistic prediction technique. It consists in quantifying the uncertainty via the dispersion in a representative ensemble of possible meteorological scenarios (hereafter identified as members). Two types of probabilistic weather forecasts are considered: ensemble nowcasts and convective-scale Ensemble Prediction Systems (EPS). Both products provide meteorological variables in a discrete way, with different time granularities, from a few minutes for the nowcast to a few hours for the EPS.

Nowcasts start from a given state of the atmosphere, for example, a storm field provided by radar information, and extrapolate their movement and their temporal development [11]. Nowcast systems work on a regional scale and are quite reliable for an hour leading time with decreasing accuracy for longer times. The meteorological information consists mainly of forecasts of the area with embedded convective cells and,

for the individual cells, their positions, extensions, strengths and heights of the clouds.

EPS are numerical weather prediction (NWP) systems which predict future atmospheric conditions by solving dynamics and physics equations that explain the movements and changes of the atmosphere. There are three main types of EPS that address different time and spatial scales in the forecast [12]: global (forecasting horizon of 3–15 days and with resolutions of between 30 and 70 km), regional (1-3 days and between 7 and 30 km), and convective-scale (1 day and between 1 and 4 km). Because of the low grid resolution of the global and regional EPS, they are not expected to predict details of small-scale systems such as thunderstorms. On the other hand, convective-scale EPS are able to resolve some of the detail of large convective systems, such as location and intensity of thunderstorms.

IV. PROBABILISTIC ANALYSIS OF SECTOR CAPACITY REDUCTION

We develop a methodology to forecast the reduction of airspace capacity under convective weather, taking into account the spatial extent and topology of the weather hazard and the traffic flow direction. We perform an analysis of ensemble capacity, including the quantification of capacity reduction as a function of forecast lead time, spatial scale and severity of the weather events.

Airspace capacity (and its reduction) is not a simple function of the weather coverage: the same percentage of airspace area covered with inclement weather may lead to drastically different possible traffic flows. Capacity estimation should consider the shape of hazardous weather cells, as well as their spatial distribution, since the airspace capacity may depend on the positions of the storms with respect to each other. For example, in Figure 1 two scenarios are shown where the same weather coverage can lead to very different capacities: on the left, a popcorn convection allows the existence of two traffic flows; while on the right, a squall line impedes the traffic from going through the sector. The geometry of the sector also plays an important role. Last but not least, the capacity depends on the direction of the flow, i.e., the source/sink edges on the boundary of the sector through which the traffic enters/exits the airspace.

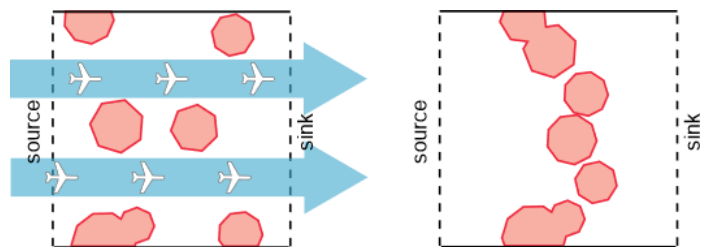


Figure 1. Same weather coverage (red polygons are hazardous weather cells) leading to different possible flows through the sector (black square).

When applying the geometric maxflow/mincut theory, a sector (on a single flight level) is represented by a 2D polygonal domain, and hazardous weather is modelled as obstacles which should be avoided by the flow (Figure 2 left). The aircraft enter

the sector through a portion of its boundary, called *source*; the aircraft exit through the portion of the boundary called *sink*. The source and the sink split the boundary of the sector into two parts called the *bottom* B and the *top* T . (If the source and sink are adjacent along the boundary, i.e., if the traffic just “clips” the sector, one of B , T may be just a point). The *critical graph* of the instance has a vertex for every obstacle, for B and for T . The edges of the graph connect all pairs of the vertices, and the weights of the edges represent the distances between the obstacles (computed using the algorithm in [13]). The *capacity of the sector* is defined by the mincut (the bottleneck for the flow) which is determined by the shortest $B - T$ path in the critical graph.

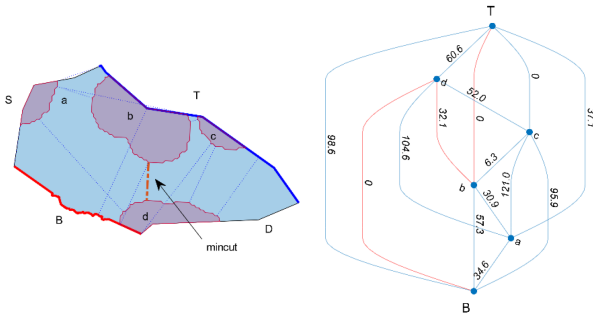


Figure 2. Left: A real example of a sector and hazardous weather cells; S and D are the source and sink (destination). Right: the critical graph with a vertex for each obstacle, bottom B and top T , weights on the edges representing the distances between the obstacles, and the shortest $B - T$ path (red), corresponding to the mincut through the sector.

The maxflow/mincut theory assumes that the flow is mostly unidirectional (single source/sink pair) because aircraft with opposing headings are vertically separated. When the sector is crossed by several flows, with different flows entering/exiting through different sources/sinks, the maxflows and the mincuts are computed separately for each source/sink pair.

Vanilla capacity estimation [1], [3] assumes that the obstacles are deterministic, i.e., that their shapes and locations were known exactly. In this paper, the capacity estimation is considered for a stochastic setting [5] when the adverse weather zones, defining the obstacles, are given by probabilistic forecasts. This extended methodology takes probabilistic weather forecasts as the input, and outputs the probability distribution of the capacity of the airspace. Unlike in [5], where the capacity reduction was estimated for a square grid cells overlaid, here we forecast the capacity reduction for real sectors in Austrian airspace.

A. Input

Our input consists of the airspace, convective weather, and flight plans.

1) *Airspace*: The airspace is a right three-dimensional prism. Following [6], we define an altitude band as a 1000ft-high horizontal slice of the airspace, centred on a flight level. Call a right prism a band prism if its bases belong to the upper and lower boundaries of a band. The airspace is split into sectors, with each sector composed of band prisms stacked one on top of another. Thus the cross-section of a sector by

any horizontal plane within an altitude band is constant; we identify the sector at the flight level with the cross-section polygon.

Figure 3 shows the sectors of a particular configuration of ATC sectors in the Austrian airspace at FL300 and FL350. At both levels, the airspace is composed of 5 sectors: N15, E15, B15, S15, and W15. The geometry of some sectors (the cross-section) may be different at different altitudes. In addition, the number of sectors may vary between the different flight levels.

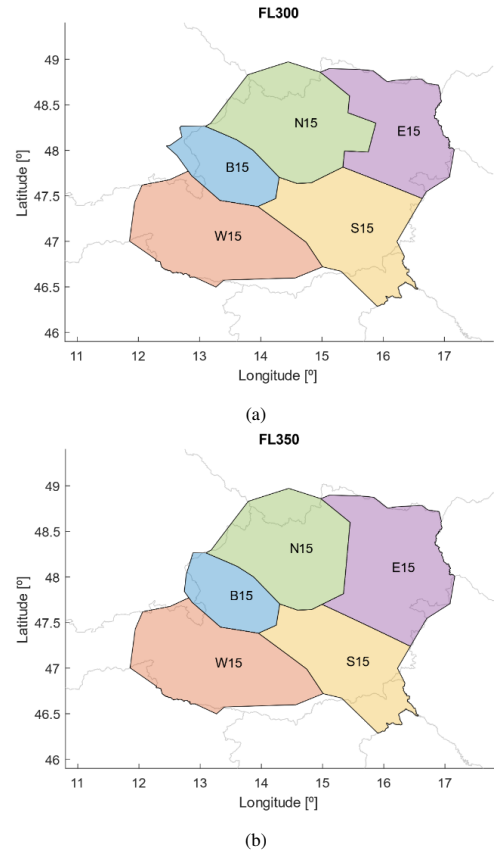


Figure 3. Example of ATC sectors in the Austrian airspace for FL300 (a) and FL350 (b).

2) *Convective Weather*: Hazardous weather cells are treated as three-dimensional obstacles to be avoided by the aircraft. The weather obstacles are provided, for each timestep over a given time horizon, by an ensemble forecast. In this work we use ensemble forecasts from different weather products: nowcast for the first hour and EPS forecast for longer-term horizon (note that the methodology applies to ensemble forecast obtained from an arbitrary weather product). For every prediction timestep, the ensemble has a member. A weather obstacle is a right prism, defined by a polygon and a vertical extent. The upper and lower bases of every obstacle are defined by an altitude band, i.e., no obstacle starts or ends inside an altitude band. This way, for a particular prediction time and an ensemble member, the hazardous weather at each altitude is a set of polygons (Figure 4).

3) *Flight plans*: The *demand* for a sector during a time interval $[t_1, t_2]$ is defined by the traffic that plan to pass through the sector. The *flight plan* for any aircraft is a sequence of 4D

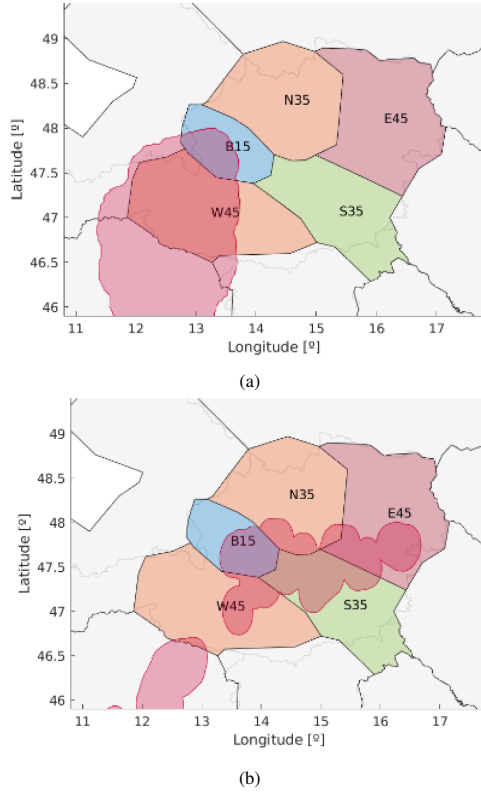


Figure 4. Example of weather-impacted regions in the Austrian airspace from nowcast (a) and EPS forecast (b).

waypoints (location and time). Note that for our analysis we need not only the total (aggregated) flow for the sector, but also the more fine-grained information on the adjacent sectors from/to which the aircraft intend to enter/exit the sector, as well as the altitude. Using the definition in [6], each flow is identified by a sector transit triplet: entry sector, current sector, and exit sector. An example is depicted in Figure 5(a), where three different flows through sector W15 (out of 20 possible flows) are shown: flow 1 (orange) corresponds to the transit triplet ACC Munchen-W15-ACC Ljubljana; flow 2 (blue) corresponds to the triplet B15-W15-ACC Padova; and flow 3 (yellow) corresponds to the triplet S15-W15-ACC Ljubljana. We calculate the *capacity* for every pair of entry/exit sectors through which the traffic intends to go. The number of aircraft in each flow is determined by identifying the sector entry and exit 4D points (time and location) of the aircraft trajectories, as well as the origin and destination adjacent sectors. Formally, for each flow j and each altitude i , an aircraft is added to the ij -th component of the demand if: 1) it flies at altitude i ; 2) it belongs to flow j ; and 3) its time within the sector, defined by the sector entry t_0 and exit time t_f , overlaps the interval $[t_1, t_2]$ (that is, $[t_1, t_2] \cap [t_0, t_f] \neq \emptyset$). Following [6], ascending or descending aircraft are treated as if they fly level at an average altitude (Figure 5(b)).

B. Available Sector Capacity Ratio

The *available sector capacity ratio (ASCR)* for each time and ensemble member is the ratio of the sector capacity under the given weather constraints to the maximum possible

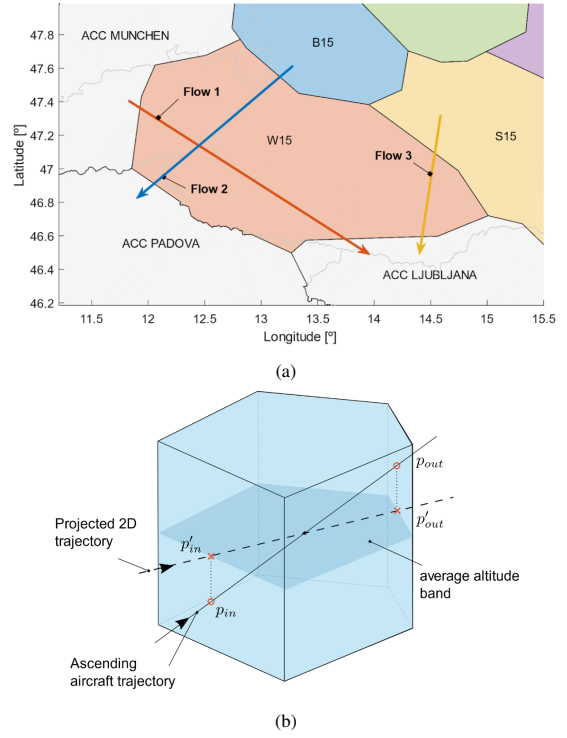


Figure 5. Example of flows through a sector in 2D (a) and the altitude band corresponding to the average of the entry and exit altitudes for ascending and descending aircraft in 3d (b).

capacity of the sector without weather systems. The ratio is a non-dimensional value ranging between 0 and 1, where 0 represents a completely blocked airspace with no usable capacity and 1 represents an airspace without constraints. ASCR is computed by averaging the capacities for all flows through the sector, as described next.

Following [6], we compute the available *flow capacity ratio (AFCR_{ij})* for every altitude band i and every pair j of entry/exit sectors. Similarly to ASCR, the available flow capacity ratio ranges from 0 to 1 and represents the ratio of the weather-impacted airspace capacity to the maximum capacity without obstacles for flow j at altitude i :

$$AFCR_{ij} = \frac{W_{ij}^{mcut}}{O_{ij}}, \quad (1)$$

where W^{mcut} is the mincut through the domain in the presence of weather obstacles and O is the mincut without obstacles (simply the distance between the bottom B and the top T of the sector, for the given altitude and entry/exit sectors pair).

After obtaining the available capacity ratio for flow j at all altitudes, the total available flow capacity ratio for flow j , $AFCR_j$, is computed as the weighted average over the altitudes:

$$AFCR_j = \sum_{i=1}^n W_{ij} * AFCR_{ij}, \quad (2)$$

where n is the number of altitude bands and the weight W_{ij} is defined as a ratio of the number of aircraft in altitude i and flow j to the total number of aircraft in flow j (if the

denominator is 0, W_{ij} is set to 0 too.) Finally, the available sector capacity ratio is determined as follows:

$$ASCR = \sum_{j=1}^F W_j * AF CR_j, \quad (3)$$

where F is the total number of flows and W_j is the weight associated with flow j , determined by the ratio of the number of aircraft in flow j to the total demand (if no aircraft pass through the sector in the considered time interval, i.e., if the total demand is 0, then W_j keeps the value from the previous time step; if no aircraft pass through the sector at the first time interval of the prediction, the values of W_j are set to $W_j = 1/F$, i.e., all flows within the sector are considered of the same weight.)

C. Probabilistic Sector Capacity Reduction

The *probability distribution* of the available sector capacity ratio for each sector is obtained by constructing and analysing the ensemble capacity forecast. For each member m of the ensemble forecast, the available sector capacity ratio $ASCR_m$ is computed. The cumulative distribution is then calculated by counting the number of ensemble members that have ASCR larger or equal to a value x and dividing by the total number of ensemble members M :

$$P(ASCR \leq x) = \frac{\sum_{m=1}^M X_m(x)}{M}, \quad (4)$$

where $X_m(x) = 1$ if $ASCR_m \leq x$, and 0 otherwise.

D. Weather-Dependent Capacity

The FMP monitors the traffic load of each ATC sector. The traffic load can be measured as the rate of flights predicted to enter the sector in a 1-hour rolling interval, i.e. the entry count. The FMP compares the traffic load with the capacity of the sector, expressed as the Monitoring Value. Next, we show how the nominal MV is reduced making use of the ASCR values previously determined.

First, let us define the time period P_k in which we want to compare the traffic load with the capacity:

$$P_k = [T_P + (k-1)\delta t, T_P + (k-1)\delta t + \Delta t], k = 1, 2, \dots, \quad (5)$$

where T_P is the time at which the prediction is performed, δt is the time step, i.e., the difference between the start times of two consecutive time periods, and Δt is the duration of each period. For example, for the entry count and the MV, it is typical to use $\delta t = 20$ min and $\Delta t = 60$ min.

Next, since the ASCRs are provided at discrete times, a right-continuous step function is created from these values: a piecewise constant function whose value at time t is the ASCR value provided for the immediately prior discrete time. For each ATC sector s and weather ensemble member m , let us denote this function as $ASCR_s^{[m]}(t)$.

Since the ASCR may take different values while in one time period P_k , we define the mean ASCR for period k , $\overline{ASCR}_{sk}^{[m]}$,

as a representative value of the sector status in that said period. It is obtained as follows:

$$\overline{ASCR}_{sk}^{[m]} = \frac{1}{\Delta t} \int_{T_P+(k-1)\delta t}^{T_P+(k-1)\delta t + \Delta t} ASCR_s^{[m]}(t) dt. \quad (6)$$

Gathering the results for all weather members, one obtains a stochastic mean status of the sector, \overline{ASCR}_{sk} , which follows a categorical distribution; its corresponding probability mass function is $p_{sk, \overline{ASCR}}(y) = 1/M$, with $y \in \{\overline{ASCR}_{sk}^{[1]}, \overline{ASCR}_{sk}^{[2]}, \dots, \overline{ASCR}_{sk}^{[M]}\}$.

The weather-dependent MV for ensemble member m , $Wx_MV_{sk}^{[m]}$, is obtained by multiplying the nominal monitoring value by the mean ASCRs:

$$Wx_MV_{sk}^{[m]} = \overline{ASCR}_{sk}^{[m]} MV_s \quad (7)$$

where MV_s is the standard MV of sector s .

Finally, gathering results for all members, as explained before, one gets the aggregated weather-dependent capacities

$$Wx_MV_{sk} = \overline{ASCR}_{sk} MV_s \quad (8)$$

When the considered time periods are long (e.g., one hour), it is common that the period P_k contains the transition time between the two weather products, T_T . When this happens, it is not possible to obtain $\overline{ASCR}_{sk}^{[m]}$ because there is no correspondence between the members of the two weather products. In that case, \overline{ASCR}_{sk} is computed in a different way. First, the mean ASCR is determined separately before and after the transition time, $\overline{ASCR}_{sk,-}$ and $\overline{ASCR}_{sk,+}$. Then, the mean ASCR for the sector is obtained as a weighted sum of the two mean ASCRs

$$\overline{ASCR}_{sk} = \frac{T_T - T_P - (k-1)\delta t}{\Delta T} \overline{ASCR}_{sk,-} + \frac{T_P + (k-1)\delta t + \Delta T - T_T}{\Delta T} \overline{ASCR}_{sk,+} \quad (9)$$

Since the two addends are independent random variables, the probability mass function of \overline{ASCR}_{sk} is obtained as the convolution of these two terms.

V. CASE STUDY

The selected case study corresponds to June 12th, 2018, a day with high convection intensity.

A. Airspace

The **Austrian airspace** under the control of ACC WIEN has been selected, which is divided into five geographical regions (B, E, N, S and W), and each region into five vertical layers (from 1 to 5). In total, 38 elementary volumes are used to define this airspace, leading to near 60 possible different ATC sectors and 190 different sector configurations. The configuration chosen is 10A1.

B. Weather

Two weather products are considered (the last available forecasts at 12:00 are used):

- **FMP-Met Ensemble Nowcast.** Observations were obtained from OPERA (Operational Programme for the Exchange of Weather Radar Information) radar composites (instantaneous surface rain rate) and SAF (Satellite Application Facilities) satellite products (convective rainfall rate and cloud top height) [14]. The Short Term Ensemble Prediction System (STEPS) method is used to generate the ensemble, composed of 15 members. We use the nowcast generated at 11:45 and interpolate it every 5 minutes. Convective cells are identified at a reflectivity of 38 dBz and enlarged with a safety margin of 13.5 NM. A common cloud top height has been also considered (flights can overfly cells with a margin of 5000 ft).
- **COSMO-D2-EPS.** Convection-permitting EPS composed of 20 members. We use the forecast generated at 09:00 and interpolate it every 15 minutes. Convective areas are identified using two convection indicators: Lifted Index (LI) and Precipitation Intensity (PI). Those areas where $LI \leq 4$ and $PI > 5$ are considered to be impermeable for the flights. As in the nowcast data, to define the weather obstacle, these impermeable areas are enlarged with an additional margin of 13.5 NM.

C. Traffic

Historic flight data (flight plans) of traffic crossing LOVV on the selected times are obtained from Eurocontrol's R&D Data Archive [15]. A total of 2961 flights are considered in the application. The traffic consists of the aircraft airborne at 12:00 or expected to take-off in the next 8 hours which plan to cross the Austrian airspace plus a surrounding area of 50 NM.

VI. RESULTS

In this section, we present an example of the resulting ASCR distribution and the corresponding reduced weather capacity for one sector (B15) of the Austrian airspace on June 12, 2018 between 12:00 and 20:00.

A. ASCR Distribution

Figure 6 shows the ASCR distribution for sector B15 for the whole period of observations. For the first hour, each boxplot represents ASCR distribution over 15 nowcast members for the 5-minutes intervals. Then, between 13:00 and 20:00, the ASCR distribution is based on COSMO-D2-EPS weather product. In the figure, each boxplot represents ASCR distribution over 20 EPS members for the 30-minutes time period. The capacity gradually decreases until 13:00, approximately, and then gradually increases.

We noted that the variance of the nowcast product generally increases with time. EPS's prediction pattern differs from that of the nowcast. The overall observation is that the nowcast data is well suited to provide a reliable basis for capacity reduction estimations, while the longer-term weather forecast products need to be advanced and adjusted to serve that purpose.

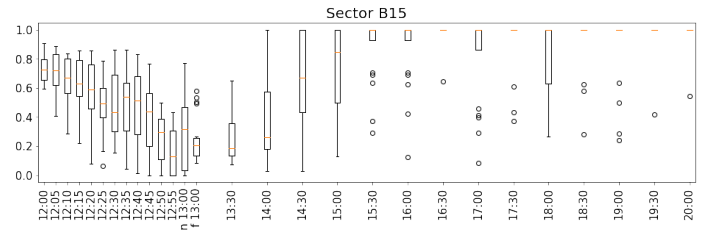


Figure 6. ASCR distribution for sector B15.

B. Reduced Weather Capacity

The weather-dependent MV, Wx_MV_{sk} , for sector B15 is shown in Figure 7 for the time periods between 12:00 and 20:00, and with $\delta t = 20$ minutes and $\Delta t = 1$ hour. The MV is represented as a heatmap, where the color for each value represents the probability of obtaining that particular value; the darker the color, the higher the probability. The 5th and 95th percentiles are represented as small black squares, and the 50th percentile (i.e., the median) as a small black diamond. The median represents the middle value, and the difference between the two percentiles is a measure of the dispersion. The nominal MV is also represented in this figure as a blue line. Regarding the median, it can be seen that the capacity starts with some reduction, it progressively further decreases during the first hour, remains at low values until 14:30, and then fully recovers, although for some weather members significant reductions may be present (as indicated by the heatmap and the 5th percentile).

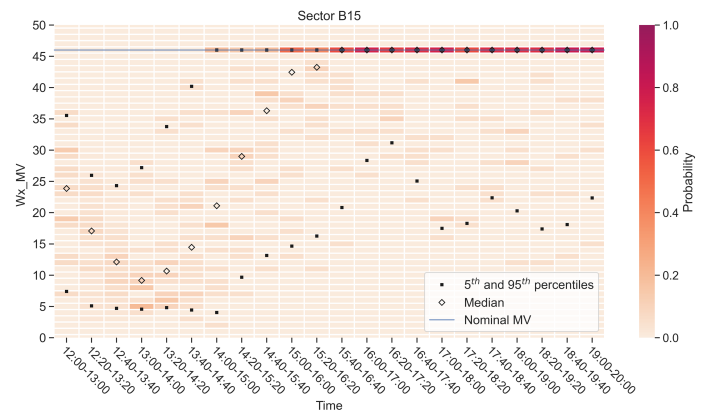


Figure 7. Weather-dependent MV for sector B15; $\delta t = 20$ minutes, $\Delta t = 1$ hour.

C. Application: Sector Congestion

Next, the probabilistic capacity reductions are applied to determine the congestion of different ATC sectors belonging to a particular sector configuration.

The probabilistic air traffic is predicted by the trajectory predictor described in [16]. This traffic is affected by the same adverse weather considered for the capacity reductions. The trajectory prediction takes into account three sources of uncertainty: 1) the meteorological uncertainty inherent to the weather forecast; 2) the operational uncertainty linked to the storm avoidance strategy; and 3) the uncertainty in the take-off

time. For different flights, it is assumed that the meteorological uncertainty is fully correlated (as they all share the same weather information) whereas the uncertainty in the initial conditions and in the operational uncertainty are statistically independent. From these flights, the entry count for ATC sector s , period k , and ensemble member m , is determined, $E_{sk}^{[m]}$, which is a probabilistic count because of the second and third sources of uncertainty. Marginalizing the entry counts from all ensemble members, one obtains the entry count of the sector, E_{sk} .

The relative difference between the entry count and the MV is known as relative overload. The relative overload for ensemble member m is obtained as:

$$ROL_{sk}^{[m]} = \frac{E_{sk}^{[m]}}{Wx_MV_{sk}^{[m]}} \quad (10)$$

Since $Wx_MV_{sk}^{[m]}$ is a deterministic value, $ROL_{sk}^{[m]}$ is just the random variable $E_{sk}^{[m]}$ scaled by $Wx_MV_{sk}^{[m]}$. Once $ROL_{sk}^{[m]}$ has been obtained, ROL_{sk} is obtained again by marginalizing over the weather ensemble members.

As previously addressed, when the period P_k encompasses the transition time between the two weather products, then $E_{sk}^{[m]}$ cannot be determined because there is no correspondence between the members of the two weather products. In that case, the entry count is determined separately before and after the transition time, and then they are added to directly determine E_{sk} . Then, ROL_{sk} is computed assuming that E_{sk} and Wx_MV_{sk} are statistically independent: $ROL_{sk} = E_{sk}/Wx_MV_{sk}$, and the probability mass function of ROL_{sk} is obtained as the Mellin convolution [17] of the numerator and the denominator.

The relative overload of sector B15 is displayed in Figure 8. The overload is certainly large for the earliest periods, which is a consequence of high counts and reduced capacities. Afterwards, the overload is reduced. For the latter periods, the median is distinctly below 1 but an overload is still possible since the 95th percentile is sometimes above 1.1. Notice that the dispersion is quite large, and the median is much closer to the 5th percentile than to the 95th one. Again, it is quite large for the first periods and smaller for the last ones. Notice that the vertical axis has been capped at 3.0 and that the 95th percentile is beyond that number for periods between 12:00 and 15:00.

Nowadays, the FMP tools to monitor the airspace use a color code to represent the congestion status of the sectors [7]:

- Green: traffic load is acceptable, up to 90% of MV.
- Yellow: traffic load is high, between 90% and 100% of MV.
- Orange: traffic load is very high, between 100% and 110% of MV.
- Red: traffic load is unacceptable, over 110% of MV.

Since the overload is now probabilistic, the color code needs to be adapted. We propose the following scheme based on two parameters: the percentiles 50 and 95 (Z_{50} and Z_{95}). The code is given by the 2-entry table shown in Figure 9. One can see that including the dispersion of the ROL distribution (off-diagonal cases) always makes the prediction more severe:

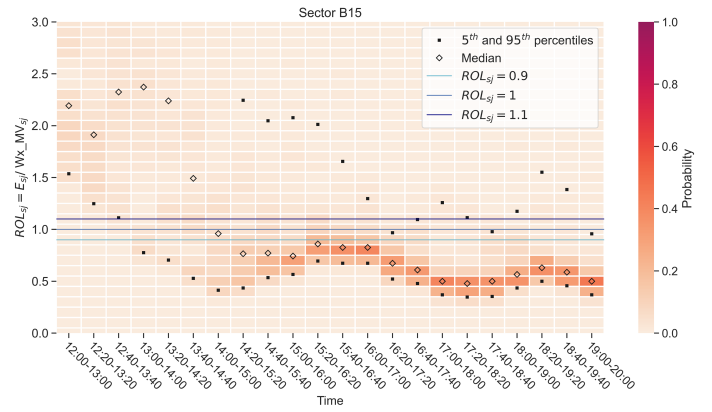


Figure 8. Entry relative overload for sector B15; $\delta t = 20$ minutes, $\Delta t = 1$ hour.

green can become yellow and even orange, yellow can become orange, and orange can become red. This is because there is a fair chance that the relative overload in these off-diagonal cases is higher than the one predicted by Z_{50} .

$Z_{50} > 110$				Red
$100 < Z_{50} \leq 110$			Orange	Red
$90 < Z_{50} \leq 100$		Yellow	Yellow	Orange
$Z_{50} \leq 90$	Green	Green	Yellow	Orange
	$Z_{95} \leq 90$	$90 < Z_{95} \leq 100$	$100 < Z_{95} \leq 110$	$Z_{95} > 110$

Figure 9. Color code for the probabilistic overload.

The status of all the sectors that make up sector configuration 10A1 is shown in Figure 10, for time periods between 12:00 and 20:00, corresponding to the entry count for 1-hour periods ($\Delta t = 1$ hour), calculated every 20 minutes ($\delta t = 20$ minutes). The status of the sector configuration is determined from the color state of its constituent sectors: green if the traffic load is acceptable for all sectors, yellow if it is high for at least one sector, orange if it is very high for at least one sector, and red if it is unacceptable for at least one sector.

In this example, most sectors present unacceptable traffic loads for some periods, and the sector configuration 10A1 is unacceptable for most of the time periods (in particular, from 12:00 until 18:00). Some sectors are overloaded at the beginning and then they recover (e.g., W3), and other sectors get overloaded between 14:00 and 16:00, approximately (e.g., S12). Sector E45 is the only one which does not become unacceptably loaded. These results indicate that traffic flow measures would be needed in this case study.

VII. CONCLUSIONS AND FUTURE WORK

We have presented a methodology for forecasting the reduction of sector capacity due to convective weather. A

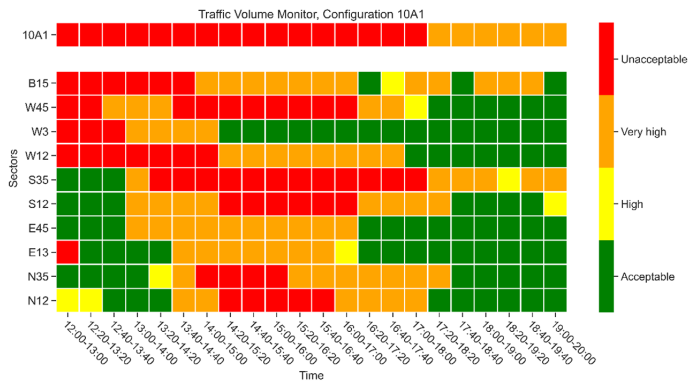


Figure 10. Congestion status for sector configuration 10A1; $\delta t = 20$ minutes, $\Delta t = 1$ hour.

probabilistic approach is used to take into account the meteorological forecast uncertainty, which is quantified using Ensemble Weather Forecasting. This methodology, based on the continuous maxflow/mincut theory, considers the spatial extent and topology of the weather hazard and the traffic flow direction. It has been applied to a realistic case study, in which the capacity reductions have been used to determine the probabilistic overload of a particular sector configuration.

The potential benefit one could expect of this methodology is the support to take anticipated, appropriate, and timely tactical flow measures under adverse weather (better-informed decision-making process for FMPs) and, as a consequence, the enhancement of ATM efficiency, which will ultimately reduce flight delays and improve passenger journeys.

The transition between the two weather products, from nowcast to EPS forecast, has resulted in discontinuities at the switching time and it has also required an adaptation of the methodologies. It is clear that a seamless weather product with an outlook horizon of several hours (8 hours in our case) would lead to smoother predictions. We believe that further investigations are needed in order to develop such a high-quality weather product and use it for probabilistic capacity estimations. We identify the development of such a probabilistic seamless product as a topic for future meteorological research.

This paper has been developed within the FMP-Met project. At the end of this project, the goal of achieving the Technology Readiness Level 1 (TRL 1) was achieved. The main step for the next phase is the development of a prototype tool, in close collaboration with FMPs, implementing the FMP-Met concept.

VIII. ACKNOWLEDGEMENT

The FMP-Met project has received funding from the SESAR Joint Undertaking (JU) under grant agreement No 885919. The JU receives support from the European Union's Horizon 2020 research and innovation programme and the SESAR JU members other than the Union.

We are grateful to the other members of the FMP-Met consortium (Agencia Estatal de Meteorología, Austrocontrol, Croacia Control, MeteoSolutions GmbH, Paris Lodron University Salzburg, Universidad Carlos III de Madrid and University of Zagreb) for their support and collaboration.

- [1] Joondong Kim, Joseph SB Mitchell, Valentin Polishchuk, Shang Yang, and Jingyu Zou. Routing multi-class traffic flows in the plane. *Computational Geometry*, 45(3):99–114, 2012.
- [2] Jimmy Krozel, Joseph SB Mitchell, Valentin Polishchuk, and Joseph Prete. Maximum flow rates for capacity estimation in level flight with convective weather constraints. *Air Traffic Control Quarterly*, 15(3):209–238, 2007.
- [3] Shang Yang, Joseph SB Mitchell, Joondong Kim, Jingyu Zou, Jimmy Krozel, and Valentin Polishchuk. Flexible airplane generation to maximize flow under hard and soft constraints. *Air Traffic Control Quarterly*, 19(3):211–235, 2011.
- [4] Joseph Mitchell, Valentin Polishchuk, and Jimmy Krozel. Airspace throughput analysis considering stochastic weather. In *AIAA Guidance, Navigation, and Control conference and exhibit*, page 6770, 2006.
- [5] Matthias Steiner, Richard Bateman, Daniel Megenhardt, Yubao Liu, Mei Xu, Matthew Pocernich, and Jimmy Krozel. Translation of ensemble weather forecasts into probabilistic air traffic capacity impact. *Air Traffic Control Quarterly*, 18(3):229–254, 2010.
- [6] Lixia Song, Craig Wanke, Stephen Zobell, Daniel Greenbaum, and Claude Jackson. Methodologies of estimating the impact of severe weather on airspace capacity. In *The 26th Congress of ICAS and 8th AIAA ATIO*, page 8917, 2008.
- [7] Kenneth Thomas. *Collaboration Human Machine Interface (CHMI) Reference Guide. Network Manager*. Eurocontrol, 8.5 edition, June 2021.
- [8] S. Niarchakou and M. Sfyroeras. *ATFCM Operations Manual. Network Manager*. Eurocontrol, 26.0 edition, April 2022.
- [9] Stephen Zobell, Craig Wanke, and Lixia Song. Probabilistic airspace congestion management. In *12th Conference on Aviation, Range, and Aerospace Meteorology (ARAM)*, American Meteorological Society, Atlanta, Georgia, 2006.
- [10] Aniel Jardines, Manuel Soler, and Javier García-Heras. Estimating entry counts and atm regulations during adverse weather conditions using machine learning. *Journal of Air Transport Management*, 95(102109):1–11, 2021.
- [11] J. W. Wilson, N. A. Crook, C. K. Mueller, J. Sun, and M. Dixon. Now-casting thunderstorms: A status report. *Bulletin of the American Meteorological Society*, 79(10):2079–2100, 1998.
- [12] World Meteorological Organization. *Guidelines on Ensemble Prediction Systems and Forecasting*. WMO-No. 1091, 2012.
- [13] Nancy M Amato. An optimal algorithm for finding the separation of simple polygons. In *Workshop on Algorithms and Data Structures*, pages 48–59. Springer, 1993.
- [14] Juan Simarro, Daniel Sacher, Ulrike Gelhardt, Javier García-Heras, Manuel Soler, Davor Crnogorac, and Markus Kerschbaum. *Deliverable 3.1. Nowcast and EPS Forecast Products*. FMP-Met Project, 00.02.00 edition, December 2020.
- [15] EUROCONTROL R&D data archive. <https://www.eurocontrol.int/dashboard/rnd-data-archive>, last accessed on 11.11.2022.
- [16] Eduardo Andrés, Javier García-Heras, Daniel González, Manuel Soler, Alfonso Valenzuela, Antonio Franco, Juan Nunez-Portillo, and Damián Rivas. Probabilistic Analysis of Air Traffic in Adverse Weather Scenarios. In *10th International Conference on Research in Air Transportation (ICRAT)*, pages 1–8, 2022.
- [17] Jacqueline Bertrand, Pierre Bertrand, and Jean-Philippe Ovarlez. The Mellin transform. *HAL open science archive*, 1995.